

Neutral Z boson pair production due to radion resonance in the Randall-Sundrum model: prospects at the CERN LHC.

Prasanta Kumar Das ¹

Chung-Yuan Christian University,
Chung-Li, Taiwan 320, Republic Of China

Abstract

The Neutral Z boson pair production due to radion resonance at the Large Hadron Collider (LHC) is an interesting process to explore the notion of warped geometry (Randall-Sundrum model). Because of the enhanced coupling of radion with a pair of gluons due to trace enomaly and top(quark) loop, the radion can provide larger event rate possibility as compared to any New Physics effect. Using the proper radion-top-antitop (with the quarks being off-shell) coupling, we obtain the correct radion production rate at LHC and explore several features of a heavier radion decaying into a pair of real Z bosons which subsequently decays into charged 4 l ($l = e, \mu$) leptons (the gold-plated mode). Using the signal and background event rate, we obtain bounds on radion mass m_ϕ and radion vev $\langle \phi \rangle$ at the 5σ , 10σ discovery level.

PACS Nos.: 11.25.Wx, 14.70.Hp.

¹Present address: Institute of Mathematical Sciences, C.I.T Campus, Taramani, Chennai 600113, India.
Electronic address: dasp@imsc.res.in

1 Introduction

The Randall-Sundrum (RS) model [1], proposed as a resolution of the well-known electroweak hierarchy problem, is particularly interesting from the phenomenological point of view [2]. According to this model, the world is 5-dimensional and the extra spatial dimension is S^1/Z_2 orbifold. The metric describing such a world can be written as

$$ds^2 = e^{-2kR_c|\theta|} \eta_{\mu\nu} dx^\mu dx^\nu - R_c^2 d\theta^2, \quad (1)$$

where k is the bulk curvature constant and R_c determines the size of the extra dimension. The variable θ parametrizes extra dimension. The model is constructed out of two D_3 branes which are located at two orbifold fixed points $\theta = 0$ and $\theta = \pi$, respectively. The brane located at $\theta = 0$ (where gravity peaks) is known as the Planck brane, while the brane located at $\theta = \pi$ [where the Standard Model (SM) fields reside and gravity is weak] is known as the TeV brane. The factor $e^{-2kR_c|\theta|}$ appearing in the metric is known as the warp factor. The length R_c , the distance between the two branes, can be related to the vacuum expectation value (vev) of some modulus field $T(x)$ which corresponds to the fluctuations of the metric over the background geometry given by R_c . Replacing R_c by $T(x)$, we can rewrite the RS metric at the orbifold point $\theta = \pi$ as

$$ds^2 = g_{\mu\nu}^{vis} dx^\mu dx^\nu \quad (2)$$

where $g_{\mu\nu}^{vis} = e^{-2\pi k T(x)} \eta_{\mu\nu} = \left(\frac{\phi(x)}{f}\right)^2 \eta_{\mu\nu}$. Here $f^2 = \frac{24M_5^3}{K}$ and M_5 is the 5-dimensional Planck scale. One is thus left with a scalar field $\hat{\phi}(x)$ [$\hat{\phi}(x) = \phi(x) - \langle \phi \rangle$] which is known as the radion field [3]. Golberger and Wise [4] proposed a mechanism for generating the potential for the field $T(x)$, with its minima at R_c which satisfies $kR_c \simeq 11 \sim 12$, a requirement for the hierarchy resolution. With this nonminimal version of the RS model with the radion $\hat{\phi}(x)$ stabilized at $\langle \phi \rangle$ via the Golberger and Wise mechanism, one can do a lot of interesting phenomenological studies. In particular, the radion, which can be lighter than the other low-lying gravitonic degrees of freedom in the RS model, will reveal itself first directly in the collider experiment or indirectly in the precision measurement and verify our notion of extra dimensions. Studies based on observable consequences of radion are available in the literature [5],[6].

Here we want to look at the pair production of Z bosons mediated by the radion at large hadron collider (LHC). The crucial roles in enhancing the signal in this channel are (a) the accessibility of the radion resonance for $m_\phi > 2m_Z$ and (b) the relatively enhanced radion coupling (due to trace anomaly and top quark loop) with a pair of gluons at LHC energies, which we will discuss in succession in later sections. Finding the radion via the above channel, the so-called *gold-plated* mode, is already available in the literatures. However some error has been translated in those studies due to the improper treatment of the Feynman rule in the radion coupling with a pair of off-shell top quarks. In the earlier studies, while estimating the radion production rate due to gluon fusion (i.e. in LHC context), radion coupling to a pair of top quarks is assumed to be proportional to the mass m_t of the top quark, which is definitely true if the produced top quarks are on-shell and obviously does not hold in the present case, since the top quarks are appearing inside the loop i.e. they are off-shell. This is the main difference between us and the already existed literatures and will be discussed in detail in Section 2.

The organization of the paper is as follows. In Sec. 2, we discuss the various interactions of the radion with the SM fields and determine the effective interaction of radion (ϕ) with a pair of gluons (g) which is due to the top loop and QCD trace anomaly. We discussed the difference in the production rate obtained by us with those already existed in the literatures. The general features of Z boson pair production via radion are discussed in Sec.3. Sec. 4 contain discussions of the predicted signals for $m_\phi > 2m_Z$, which is followed by the background estimate. We conclude in Sec. 5

2 Effective interaction of radion with the SM fields

Radion interactions with the SM fields confined on the TeV brane are governed by 4-dimensional general covariance. It couples to the trace of the energy-momentum tensor of the SM fields in the following manner:

$$\mathcal{L}_{int} = \frac{\hat{\phi}}{\langle \phi \rangle} T_\mu^\mu(SM), \quad (3)$$

where $\langle \phi \rangle$ is the radion vev. The trace of the energy-momentum tensor of the SM fields is given by

$$T_\mu^\mu(SM) = \sum_\psi \left[\frac{3i}{2} (\bar{\psi} \gamma_\mu \partial_\nu \psi - \partial_\nu \bar{\psi} \gamma_\mu \psi) \eta^{\mu\nu} - 4m_\psi \bar{\psi} \psi \right] - 2m_W^2 W_\mu^+ W^{-\mu} - m_Z^2 Z_\mu Z^\mu + (2m_h^2 h^2 - \partial_\mu h \partial^\mu h) + \dots \quad (4)$$

The photon and the gluons couple to the radion via the usual top loop diagrams. *It is important to note at this point that as long as the fermions (produced from the decay of radion) are on-shell, their couplings are exactly same as the SM Higgs boson i.e. proportional to the fermion mass and this makes it very difficult to isolate radion from the Higgs boson by studying the final state decay products. However, if they are off-shell (e.g. radion production via top loop in gluons fusion), the situation is different due to the kinetic term of $\phi - t - \bar{t}$ coupling term in the kinetic energy part of the Lagrangian (see the discussion in section 2.1). Considering the correct Feynman rule for $\phi - t - \bar{t}$ coupling [i.e. the kinetic term (missing in the literature) along with the mass term (present in the literature)] and thus finding the correct radion production due to top loop in gluon fusion in the present context, differs crucially from those already existed in the literature [5].* Besides the top loop, an added source of enhancement of radion production in gluon fusion is the QCD trace anomaly, which we discuss below. For the sake of completeness, we first derive the lagrangian comprising radion-top coupling and then discuss the effective radion-gluon coupling which is due to top loop and trace anomaly.

2.1 Lagrangian for the radion-top coupling

The radion coupling to the top quark in the Randall-Sundrum model can be derived from the following action

$$S_1 = \int d^4x \sqrt{-g_{vis}} \left[\bar{\psi} (i\gamma_a e^{a\mu} D_\mu - m) \psi \right]. \quad (5)$$

Note that the action (Eq. (5)) should also contain the Yukawa term $\frac{g_t}{\sqrt{2}} H \bar{\psi} \psi$ with H being the SM Higgs field. Such a Yukawa term is irrelevant for the present study and we will not consider this any further. The field $e^{a\mu}$ is the contravariant vierbein field for the visible brane

and g_{vis} is the determinant of the metric $g_{\mu\nu}^{vis}$ (Eq. (2)). In the presence of radion fluctuation it satisfies the normalization condition

$$e^{a\mu} e_a^\nu = g^{\mu\nu} = \left(\frac{\phi}{f}\right)^{-2} \eta^{\mu\nu} = e^{2\pi k T(x)} \eta^{\mu\nu}. \quad (6)$$

D_μ is the covariant derivative with respect to general coordinate transformation and is given by

$$D_\mu \psi = \partial_\mu \psi + \frac{1}{2} w_\mu^{ab} \Sigma_{ab} \psi.$$

w_μ^{ab} is the spin connection and it can be computed from the vierbein fields by using the relation

$$w_\mu^{ab} = \frac{1}{2} e^{\nu a} (\partial_\mu e_\nu^b - \partial_\nu e_\mu^b) - \frac{1}{2} e^{\nu b} (\partial_\mu e_\nu^a - \partial_\nu e_\mu^a) - \frac{1}{2} e^{\rho a} e^{\sigma b} (\partial_\rho e_{\sigma c} - \partial_\sigma e_{\rho c}) e_\mu^c, \quad (7)$$

where Σ_{ab} is given by the expression $\Sigma_{ab} = \frac{1}{4} [\gamma_a, \gamma_b]$. In the presence of radion fluctuations on the visible brane, the spin connection is given by

$$w_\mu^{ab} = \frac{1}{\phi} \partial_\nu \phi [e^{\nu b} e_\mu^a - e^{\nu a} e_\mu^b]. \quad (8)$$

The covariant derivative of the fermion field then becomes

$$D_\mu \psi = \partial_\mu \psi + \frac{1}{4\phi} \partial^\nu \phi [\gamma_\mu, \gamma_\nu] \psi,$$

where the γ_μ are independent of space time coordinates. The action that determines the radion couplings to top quark can therefore be written as

$$\begin{aligned} S_1 &= \int d^4x \left(\frac{\phi}{f}\right)^4 \left[\left(\frac{\phi}{f}\right)^{-1} \bar{\psi} \{i\gamma^\mu \partial_\mu + \frac{3i}{2\phi} \partial_\mu \phi \gamma^\mu\} \psi - m_t \bar{\psi} \psi \right] \\ &= \int d^4x \left[\bar{\tilde{\psi}} \{i\gamma^\mu \partial_\mu \tilde{\psi} + \frac{3i}{2\phi} \partial_\mu \phi \gamma^\mu \tilde{\psi}\} \left(1 + \frac{\hat{\phi}}{\langle\phi\rangle}\right)^3 - \tilde{m}_t \left(1 + \frac{\hat{\phi}}{\langle\phi\rangle}\right)^4 \bar{\tilde{\psi}} \tilde{\psi} \right] \\ &= \int d^4x \left[\bar{\tilde{\psi}} i\gamma^\mu \partial_\mu \tilde{\psi} - \tilde{m}_t \bar{\tilde{\psi}} \tilde{\psi} \right] + \int d^4x \left[\frac{3i}{\langle\phi\rangle} \bar{\tilde{\psi}} \gamma^\mu \partial_\mu \tilde{\psi} \hat{\phi} + \frac{3i}{2\langle\phi\rangle} \bar{\tilde{\psi}} \gamma^\mu \tilde{\psi} \partial_\mu \hat{\phi} - 4\tilde{m}_t \frac{\hat{\phi}}{\langle\phi\rangle} \bar{\tilde{\psi}} \tilde{\psi} \right] + \dots \quad (9) \end{aligned}$$

We keep terms containing one $\hat{\phi}$ field [the second term in the last line of Eq. (9)] which gives rise to the radion-top interaction with the following Feynman rule:

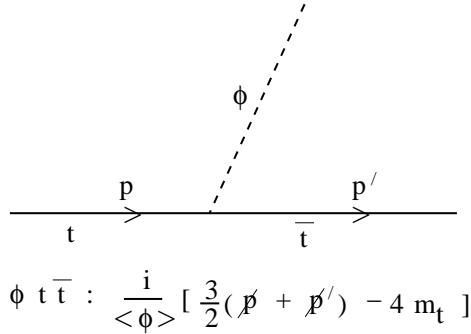


FIG. 1. Feynman diagrams for the radion coupling with a pair of top quarks.

$$\frac{i}{\langle \phi \rangle} \left[\frac{3}{2} (\not{p} + \not{p}') - 4 m_t \right], \quad (10)$$

where p, p' correspond to four-momenta of t and \bar{t} quarks (see Fig. 1) and m_t , the top quark mass. Note that if the top quarks are on-shell, the above Feynman rule can be shown (using the equation of motion) to be equal to $-i \frac{m_t}{\langle \phi \rangle}$ similar to the corresponding SM Higgs boson coupling: $-i \frac{m_t}{v}$ where the electro weak vev $v = 247$ GeV. These two couplings are exactly identical in the limit $\langle \phi \rangle \rightarrow v$. In Eq. (9) the Ellipsis (\cdots) corresponds to terms involving two,three $\hat{\phi}$ fields [see [7] for the details]. Note that in the above $\psi = \left(\frac{f}{\langle \phi \rangle} \right)^{3/2} \tilde{\psi}$, and $m_t = \left(\frac{f}{\langle \phi \rangle} \right) \tilde{m}_t$. In the following, we shall assume that all fields and parameters have been properly scaled so as to corresponds to the TeV scale and drop the *tilde* sign.

2.2 Effective radion-gluon coupling: QCD anomaly and top loop

2.2.1 QCD anomaly at order α_s

The radion couples to the trace of the energy-momentum tensor ($T_{\mu\nu}$), which can be equated with the four-divergence of the dilatation current (D_μ) associated with scale symmetry of the theory i.e.

$$\partial^\mu D_\mu = \partial^\mu (T_{\mu\nu} \delta x^\nu) = T_\mu^\mu.$$

Scale symmetry is a good symmetry at the classical level (i.e. $\partial^\mu D_\mu = T_\mu^\mu = 0$) in the limit of zero mass and in the absence of dimensionful couplings. However, quantum correction breaks the scale invariance and the divergence of the dilatation current receives the anomalous contribution given by $\partial^\mu D_\mu = T_\mu^\mu \neq 0$. Such a non-zero anomalous T_μ^μ generated due to

the quantum correction (zero at the classical level), is known as the *Trace Anomaly* or *Weyl Anomaly* term and it can be shown to be proportional to the relevant beta function of the underlying gauge theory [8]. The radion coupling to the massless gluons (or photons) is crucially controlled by such a trace anomaly term. For gluons, the interaction lagrangian due to this trace anomaly term can be written as

$$T_\mu^\mu (SM)^{anom} = \sum_a \frac{\beta_s(g_s)}{2g_s} G_{\mu\nu}^a G^{a\mu\nu}, \quad (11)$$

where g_s is the strong coupling constant and $\beta_s(g_s)/2g_s = -[\alpha_s/8\pi] b_{QCD}$. Here $b_{QCD} = 11 - 2n_f/3$ and n_f is the number of quark flavours.

2.2.2 Top loop at order α_s

At order α_s , a radion can couple to a pair of gluons via the one-loop diagrams of Fig. 2. We follow the usual [9] procedure to evaluate the amplitude for the process $\phi \rightarrow gg$. Consistency with the Lorentz invariance and the transverse nature of the gluon [i.e. $P^\mu \varepsilon_\mu^{a*}(P) = Q^\nu \varepsilon_\nu^{a*}(Q) = 0$] leads to the following form of the amplitude:

$$\begin{aligned} \mathcal{M}[\phi(k) \rightarrow g(P)g(Q)] &= M^{\mu\nu} \varepsilon_\mu^{a*}(P) \varepsilon_\nu^{b*}(Q) \\ &= [F_1(k^2) P^\nu Q^\mu + F_2(k^2) \eta^{\mu\nu}] \varepsilon_\mu^{a*}(P) \varepsilon_\nu^{b*}(Q) \end{aligned} \quad (12)$$

with $\eta_{\mu\nu} = \text{diag}(1, -1, -1, -1)$ and $k = P + Q$. Imposition of the current conservation $Q_\nu M^{\mu\nu} = 0$ (follows from the gauge symmetry) relates the two form factors as

$$F_2(k^2) = -P.Q F_1(k^2). \quad (13)$$

Inserting this in Eq.(12), we find the amplitude $\mathcal{M}(\phi \rightarrow gg)$ as

$$\mathcal{M}(\phi \rightarrow gg) = F_1(k^2) [P^\nu Q^\mu - P.Q \eta^{\mu\nu}] \varepsilon_\mu^{a*}(P) \varepsilon_\nu^{b*}(Q). \quad (14)$$

We now evaluate the set of diagrams of Fig. 2 and find $F_1(k^2)$ as

$$\frac{\alpha_s(\mu^2) \delta_{ab} Q_f^2}{2\pi \langle \phi \rangle} I_{QCD}, \quad (15)$$

where Q_f is 2/3 for the top quark. Diagrams 2(c) and 2(d) do not give rise to contributions of the form Eq. (14), a necessary requirement which follows from the gauge invariance and other constraints (discussed above). Thus their contributions to the effective $\phi - g - g$ interaction, are simply zero. Only diagrams 2(a) and 2(b) contribute.

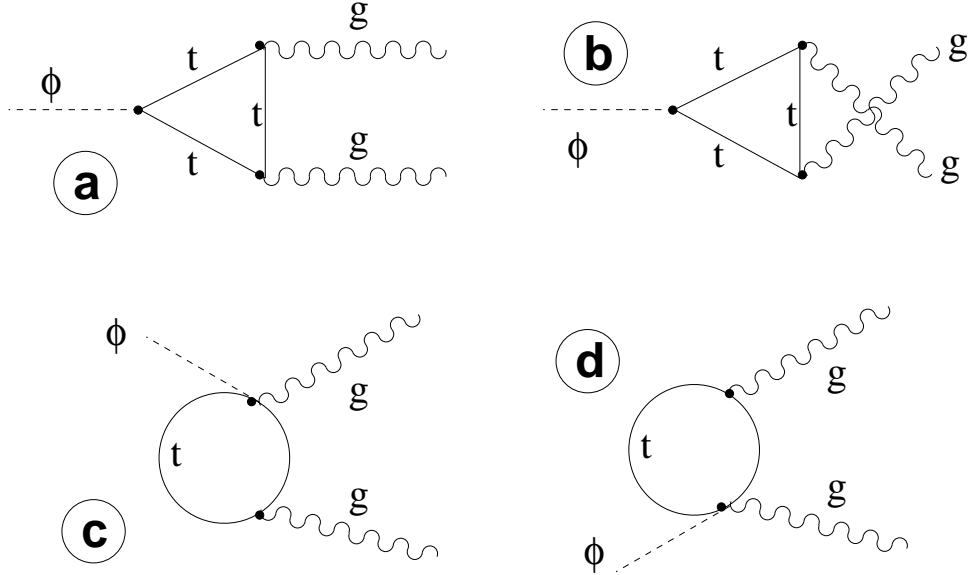


FIG. 2. Feynman diagrams with a top quark loop contributing to the process $\phi \rightarrow gg$ at order α_s .

The loop function I_{QCD} arising in the process is given by

$$\begin{aligned} I_{QCD} &= - \left[20 - 12\sqrt{x_t - 1} \lambda(x_t) - 2(4x_t - 1)\lambda^2(x_t) \right] \quad \text{for } x_t > 1, \\ &= - \left[20 - 12\sqrt{1 - x_t} \lambda(x_t) - 2(1 - 4x_t)\lambda^2(x_t) \right] \quad \text{for } x_t \leq 1, \end{aligned} \quad (16)$$

where $x_t = 4m_t^2/m_\phi^2$ and m_ϕ is the radion mass. Note the presence of the constant term and the term linear in $\lambda(x_t)$ arising in the loop function. They, found to be absent in the literature [5], arises due to the presence of the kinetic term in the $\phi - t - \bar{t}$ coupling. As we will see, this results in an important role in the radion production rate. The function $\lambda(x_t)$ is given by

$$\begin{aligned} \lambda(x_t) &= \tan^{-1} \left(\frac{1}{\sqrt{x_t - 1}} \right) \quad \text{for } x_t > 1, \\ &= \frac{1}{2} \left[\ln \left(\frac{1 + \sqrt{1 - x_t}}{1 - \sqrt{1 - x_t}} \right) - i\pi \right] \quad \text{for } x_t \leq 1. \end{aligned} \quad (17)$$

Note that for $x_t > 1$, $n_f = 5$, so b_{QCD} [arising in the trace anomaly term (see Sec. 2)] is $23/3$, while for $x_t \leq 1$, $n_f = 6$ and $b_{QCD} = 21/3$. Note that the $x_t \leq 1$ i.e. $m_\phi \geq 2m_t$, corresponds to the top resonance inside the loop and is the region where the heavy quark approximation breaks down.

On the whole, the effective $\phi-g-g$ interaction finds contributions from the trace anomaly and the top quark loop and hence, can be written as

$$\frac{i\alpha_s(\mu^2)\delta_{ab}}{2\pi\langle\phi\rangle} \left[b_{QCD} + Q_f^2 I_{QCD} \right] [P^\nu Q^\mu - P.Q\eta^{\mu\nu}]. \quad (18)$$

With the above interactions, we calculate the decay width $\Gamma[\phi \rightarrow gg]$ as

$$\Gamma[\phi \rightarrow gg] = \frac{\alpha_s^2(\mu^2)m_\phi^3}{32\pi^3\langle\phi\rangle^2} |b_{QCD} + Q_f^2 I_{QCD}|^2. \quad (19)$$

Radion decay to other SM fields have been discussed in Refs. [5, 10].

3 Neutral Z boson pair production: LHC prospects

The neutral Z boson pair production from gluon-gluon fusion at the LHC has been extensively studied in the context of the SM as well as several of its extensions such as the minimal supersymmetric standard model (MSSM). A precise estimate for the Z boson pair production due to Higgs resonance and a detailed analysis of it's subsequent decay into charged leptonic final states is available in the literature [11]. Any excess over this can be interpreted as the signature of new physics [12]. The mediation of the heavier neutral Higgs in supersymmetry has been shown to be the source of some enhancement in a region of the parameter space. Theories with extra dimensions, too, have been explored in this context, both in the ADD (Arkani-Hamed, Dimopoulos and Dvali [13]) and RS models [14]. It has been reported in these papers that the mediation of gravitons can boost the Z boson pair production rates. In this paper we wish to emphasize that the presence of a stabilized radion in the nonminimal RS context is particularly significant. This is because (i) *whereas the graviton resonance in the RS scenario is usually at too high a mass to be significant, a relatively less massive radion can be within the kinematic reach*, and also (ii) *the enhancement of radion coupling to a pair of gluons via the trace anomaly term and top loop picks up the contributions*. We have computed the predicted rates for the case $m_\phi > 2m_Z$ and analyzed the viability of the resulting signals with appropriate event selection strategies.

Using Breit-Wigner approximation for the resonant production of a radion, one finds the following expression for the cross section for $pp \rightarrow \phi \rightarrow ZZ$ (the dominant partonic subprocess

being $gg \rightarrow \phi \rightarrow ZZ$):

$$\sigma_{ZZ}(pp \rightarrow \phi \rightarrow ZZ) = \int dx_1 \int dx_2 g_1(x_1, Q^2) g_2(x_2, Q^2) \hat{\sigma}_{ZZ}(gg \rightarrow \phi \rightarrow ZZ), \quad (20)$$

where

$$\begin{aligned} \hat{\sigma}_{ZZ}(gg \rightarrow \phi \rightarrow ZZ) &= \frac{\alpha_s^2(\mu^2)}{2048 \pi^3 \langle \phi \rangle^4} |b_{QCD} + Q_f^2 I_{QCD}|^2 \frac{\hat{s}[\hat{s}^2 - 4m_Z^2 \hat{s} + 12m_Z^4]}{[(\hat{s} - m_\phi^2)^2 + m_\phi^2 \Gamma_\phi^2]} \\ &= \frac{\Gamma[\phi \rightarrow gg]}{64 m_\phi^3 \langle \phi \rangle^2} \frac{\hat{s}[\hat{s}^2 - 4m_Z^2 \hat{s} + 12m_Z^4]}{[(\hat{s} - m_\phi^2)^2 + m_\phi^2 \Gamma_\phi^2]}, \end{aligned} \quad (21)$$

In obtaining Eq.(21), we made use the decay width of radion (ϕ) into a pair of gluons (g) i.e. $\Gamma[\phi \rightarrow gg]$ and assumes the validity of time reversal symmetry. Here \hat{s} ($= x_1 x_2 s$) is the centre-of-mass energy for the partonic subprocess, \sqrt{s} ($= 14$ TeV) corresponds to the proton-proton centre-of-mass energy, $g_1(x_1, Q^2)$ and $g_2(x_2, Q^2)$ are the gluon distribution functions of the two colliding protons, x_1 and x_2 are the momentum fractions of the partons (gluons) of the colliding protons and m_ϕ and Γ_ϕ denotes the mass and total decay width of the radion. The factorization scale Q^2 and renormalization scale μ^2 appearing in $g(x, Q^2)$ and $\alpha_s(\mu^2)$ are fixed at $Q^2 = \mu^2 = \hat{s}$ in our analysis. We have used CTEQ4L [15] parton distribution functions, setting the renormalisation scale at the partonic subprocess centre-of-mass energy ($\sqrt{\hat{s}}$). We have checked that the predicted results are more or less unchanged if this scale is set at radion mass (m_ϕ).

In Eq. (21), we find that away from the radion resonance, the term proportional to Γ_ϕ^2 is of little consequence, and the total rate falls as $1/\langle \phi \rangle^4$. This is because the decay width of the radion in any channel is proportional to $1/\langle \phi \rangle^2$. Near resonance, on the other hand, the contribution is dictated by the term with Γ_ϕ in the radion propagator. Since, in the narrow width approximation, one can write $1/[(\hat{s} - m_\phi^2)^2 + m_\phi^2 \Gamma_\phi^2] \simeq \pi \delta(\hat{s} - m_\phi^2)/m_\phi \Gamma_\phi$, the overall rate falls as $1/\langle \phi \rangle^2$ near resonance.

4 Numerical Analysis

4.1 Event selection and results: $m_\phi > 2m_Z$

The signal of Z -pair production due to radion resonance depends on the final states produced by the decay of Z -boson. In our analysis, we consider the mass range $m_\phi > 2m_Z$ and in

such a case, the $BR(\phi \rightarrow b\bar{b})$ falls to 0.0028 i.e. $\sim 3\%$ (say at $m_\phi = 200$ GeV) and hence the $b\bar{b}$ mode for detecting the radion resonance, is not worthwhile to look. On the other hand for the same m_ϕ value, the $BR(\phi \rightarrow ZZ)$ becomes 13%, and can be considered as quite useful for detecting the radion resonance. We will consider the scenario in which the produced Z will decay mainly leptonically (i.e. $l = e, \mu$). So, the final state contains 4 charged leptons and normally such events may have appreciable SM background arising from the following sources:

- The electro weak production of $l^+l^-l^+l^- (l = e, \mu)$,
- Higgs production due to gluons fusion, which after subsequent decay into 2 Z bosons can produce 4 charged leptons in the final state. This is the dominant background process.

However, using a proper set of cuts one can diminish this background effect, thereby, enhancing the signal. The cuts used in our analysis can be listed as follows:

- Each of the produced charged lepton (e or μ type) must have the pseudorapidity η satisfying $-3 < \eta < 3$.
- Each of the produced charged lepton must have transverse momenta p_T greater than 15 GeV.

After applying all the above cuts, the cross section for the process $pp(gg) \rightarrow \phi \rightarrow ZZ \rightarrow l^+l^-l^+l^-$ (the signal) and $pp(gg) \rightarrow h \rightarrow ZZ \rightarrow l^+l^-l^+l^-$ and $pp(gg) \rightarrow (EW, non-resonant) \rightarrow l^+l^-l^+l^-$ (the backgrounds) are obtained. In Fig. 3 we have plotted these cross sections for the signal and background against m_S (GeV). For the signal $m_S = m_\phi$ and $\langle \phi \rangle = 250, 500, 750, 1000$ GeV with the SM Higgs mass $m_h = 185$ GeV. For the background $m_S = m_h$ for the resonating Higgs channel, besides other non-resonating electro weak channels. We considered the cases in which Z decay into electrons and muons ($l = e, \mu$) with total branching ratios 0.0682. In addition, an average detection efficiency of 80% per lepton has been assumed. Below, we make the following observations

- From Fig. 3, we see that there is a substantial enhancement of the rates (signal) in comparison to what is obtained in the Standard Model. The bump at around $M_S =$

350 GeV, resembles the top resonance inside the top loop (the scalar (radion/Higgs) production channel via gluon fusion). Such a top resonance, encoded in the function $\lambda(x_t)$ (see Eq.(16)) and appearing in the loop integral, seems to happen at $m_S \geq 2m_t$ which is being manifested in the imaginary part of the $\lambda(x_t)$ function (Eq.(17)).

An estimate of the signal and background event rate (obtained by multiplying the cross section with the integrated luminosity) is given in Table 1 and 2.

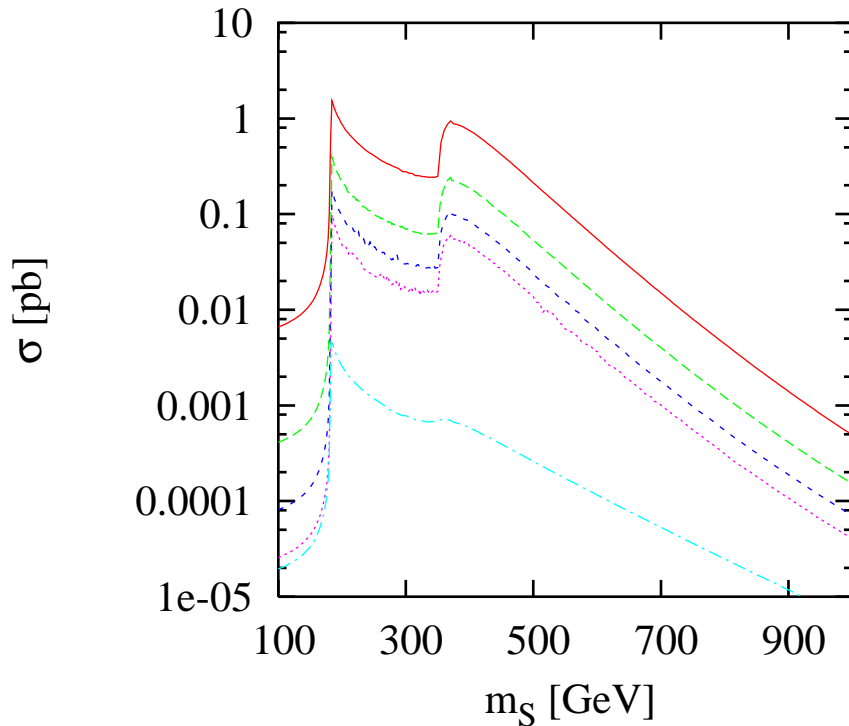


FIG. 3 (color online): *Plots showing the total cross section of 4 $l(l = e, \mu)$ in pp collisions due to radion resonance as a function of the scalar(S) mass m_S , with S is ϕ and h for the signal and the background, respectively. For the signal, we choose the SM Higgs mass $m_h = 185$ (GeV) and $\langle\phi\rangle = 250$ (solid curve), 500 (long-dashed curve), 750 (short-dashed curve) and 1000 (dotted curve) (GeV). The lower (dashed-dotted) curve corresponds to the SM background. We choose $Q^2 = \mu^2 = \hat{s}$, although the result remains more or less unchanged if one chooses $Q^2 = \mu^2 = m_\phi^2$.*

- From Fig. 3 and Table 1, it is clear that the total cross section (and hence the event rate) of the signal falls with the increase in $\langle\phi\rangle$, i.e. near resonance it goes as $\frac{1}{\langle\phi\rangle^2}$ while

away from the resonance it goes as $\frac{1}{\langle\phi\rangle^4}$ (see also the discussion of Sec. 3).

- Figure 3 (see also Table 1) shows that, for a given $\langle\phi\rangle$, the cross section falls with the increase in m_ϕ [see Eqs.(20) and (21)].
- The total event(signal) rate is greater than that predicted in ADD and RS scenario involving spin-2 gravitons. As has been mentioned before that this enhancement is due to two reasons, namely, (a) possibility of having a radion resonance and (b) the enhanced coupling at radion-gluon-gluon vertex due to trace anomaly and top loop. It is worthwhile to give some number related to the signal cross section which differs from the literatures, say, Chaichian *et. al.* in the $\xi = 0$, where ξ is the radion-Higgs mixing parameter [5] and as we mentioned earlier that such difference is due to the treatment of the $\phi - t - \bar{t}$ coupling required in the triangle top loop evaluation. For example, below $2m_t$ threshold, say at around $m_\phi = 200$ GeV, we find $\sigma = \sigma_s = 0.047$ pb in contrast to ~ 0.01 pb (Chaichian *et. al.*) for the radion vev $\langle\phi\rangle$ about 1 TeV. Above $2m_t$ threshold, with the same $\langle\phi\rangle$ value, say at $m_\phi = 370$ GeV, we find the signal cross section σ about 0.06 pb, whereas they found 0.025 pb.

Table 1: Showing the event (signal) rate as a function of radion mass m_ϕ and vev $\langle\phi\rangle$.

m_ϕ (GeV)	$\langle\phi\rangle$ (GeV)	σ_s (fb)	\mathcal{L} (fb^{-1}/yr)	Events/yr
250	250	408	100	40800
	500	100	100	10000
	750	45	100	4500
	1000	22	100	2200
500	250	213	100	21300
	500	53	100	5300
	750	24	100	2400
	1000	14	100	1400

Table 2: Background(bgd) event rate estimation with the assumption that the dominant contribution comes from the SM Higgs (with $m_h = 185$ GeV) resonance due to gluon-gluon fusion.

$\sigma_B(fb)$	$\mathcal{L} (fb^{-1}/yr)$	Events(bgd)/yr
4.4	100	440

- A bump at around $m_\phi = 350$ GeV corresponds to the top resonance inside the top loop. Above this resonance (the $2m_t$ threshold), the cross section is mainly dominated by the top loop. Note that, before this resonance, the large signal cross section was mainly due to trace anomaly, which remains important even after this $2m_t$ threshold.
- While maintaining the fact that the signal cross section be greater than that of the SM background, one can even allow larger m_ϕ values corresponding to lighter $\langle\phi\rangle$ choices, the feature which will be explored in the next section.

4.2 Significance contours

With an integrated luminosity of $100\ fb^{-1}$, the above rate indicate a rather impressive prospect of detecting the radion resonance via the pair-produced Z bosons and it's subsequent charged leptonic decays. To gauge the situation, however, one should also remember that the backgrounds, even after applying proper set of cuts, are never totally eliminated and one can compare the signal with this background. In Fig. 4, we show the contour plots in the plane of radion mass m_ϕ and radion vev $\langle\phi\rangle$ corresponding to $\frac{S}{\sqrt{B}} (= R_{SB}) = 5, 10$, where S and \sqrt{B} are the number of events corresponding to the signal and the background with the above luminosity. In calculating the backgrounds, we have taken both statistical and systematic effects into account, assuming the systematic uncertainty to be 2% of the total background and adding it in quadrature to the computed background itself. For each curve in Fig. 4, the region above the curve is allowed. For example, for an intermediate (heavy) m_ϕ , say about 250 (500) GeV, we find lower bounds on $\langle\phi\rangle$ about ~ 2741 (778) GeV corresponding to $R_{SB} = 5$ and ~ 2076 (~ 556) GeV corresponding to $R_{SB} = 10$. These plots

corresponds to finding the signal over a large region of the parameter space and suggests the possibility of having a heavier radion mass with a moderately lower radion vev $\langle\phi\rangle$, although the possibility of having an intermediate radion mass is not ruled out.

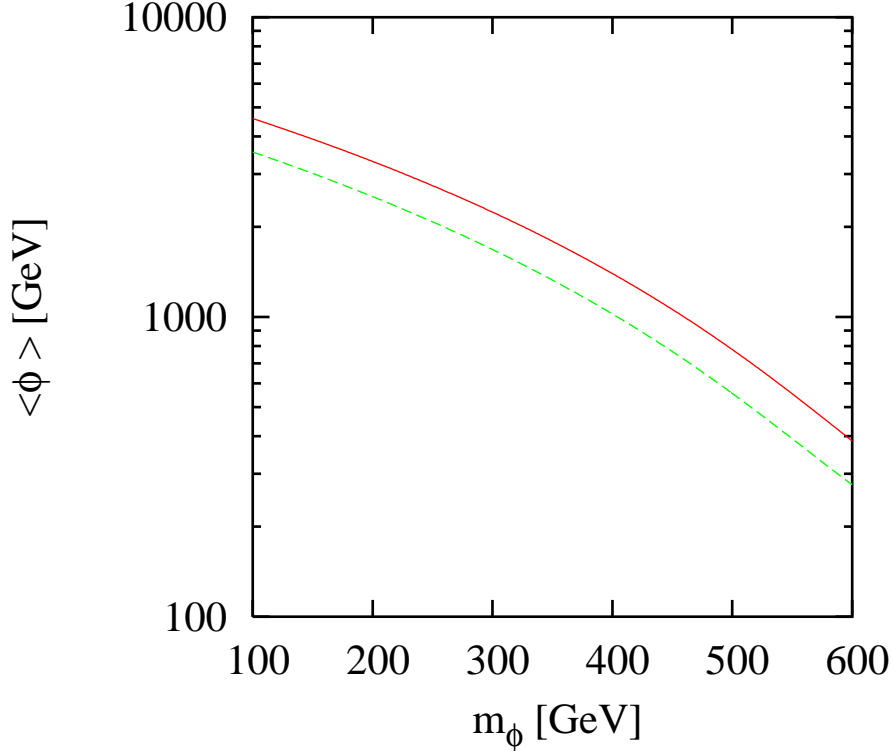


FIG. 4 (color online). *Contour plot in the plane of m_ϕ and $\langle\phi\rangle$ corresponding to $R_{SB} = 5$ (solid line) and 10 (dashed line).*

5 Summary and Conclusion

The enhanced coupling of the radion-gluon-gluon due to top loop and trace anomaly offers an immense possibility of finding radion at Large Hadron Collider. We have considered the correct radion-top-antitop coupling and fix the radion production rate at LHC. We have considered the channel in which the radion is produced as a resonance in gluon-gluon fusion and then decay to a pair of Z bosons, which subsequently decays into 4 charged leptons, $l (= e, \mu)$. The SM background comprising 4 l final sets is found to be smaller than that due to the signal (radion resonance) even after applying a proper set of cuts for a wide range of

radion mass (m_ϕ) values. For m_ϕ ranging from 180 to 1000 GeV, the signal cross section dominates over that due to SM background. Exploiting the signal and background ratio, we make the contour plots in $m_\phi - \langle \phi \rangle$ plane. The contour plot suggests the possibility of having an intermediate to heavier radion of mass about ~ 250 (500) GeV with $\langle \phi \rangle$ about 2076 (556) GeV at the 10σ discovery level.

Acknowledgement

I thank Prof. U. Mahanta (deceased) and Prof. S. Raychaudhuri for introducing me to brane world phenomenology and Prof. Pankaj Jain for his very useful comments and suggestions after reading this manuscript. Special thanks are reserved for Prof. Kwei-Chou Yang who provided me a nice stay with NSC support at CYCU, Taiwan, where this work was finally completed.

References

- [1] L. Randall and R. Sundrum, *Phys. Rev. Lett.* **83**, 3370 (1999); **83**, 4690 (1999).
- [2] M. L. Graesser, *Phys. Rev.* **D 61**, 074019 (2000); S. C. Park and H. S. Song, *Phys. Lett.* **B 506**, 99 (2001); C. S. Kim, J. D. Kim and J. Song, *Phys. Lett.* **B 511**, 251 (2001).
- [3] G. F. Giudice, R. Rattazzi and J. D. Wells, *Nucl. Phys.* **B 595**, 250 (2001); W. D. Goldberger and M. B. Wise, *Phys. Lett.* **B 475**, 275-279 (2000); W. D. Goldberger and I. Z. Rothstein, *Phys. Lett.* **B 491**, 339 (2000).
- [4] W. D. Goldberger and M. B. Wise, *Phys. Rev. Lett.* **83**, 4922 (1999); W. D. Goldberger and M. B. Wise, *Phys. Rev.* **D 60**, 107505 (1999).
- [5] K. Cheung, *Phys. Rev.* **D 63**, 056007 (2001); M. Chaichian *et. al.*, *Phys. Lett.* **B 524**, 161 (2002), hep-ph/0110035; C. Csaki, M. Graesser, L. Randall and J. Terning, *Phys. Rev.* **D 62**, 045015 (2000); U. Mahanta and A. Datta, *Phys. Lett.* **B 483**, 196 (2000); U. Mahanta and S. Rakshit, *Phys. Lett.* **B 480**, 176 (2000); S. Bae, P. Ko, H. Lee and J. Lee, *Phys. Lett.* **B 487**, 299 (2000).

- [6] P. K. Das and U. Mahanta, *Phys. Lett.* **B 520**, 307 (2001), *Phys. Lett.* **B 528**, 253 (2002), *Mod. Phys. Lett.* **A 19**, 1855 (2004), *Nucl.Phys.* **B 644**, 395 (2002); M. Chaichian, A. Datta, K. Huitu and Z. Yu, *Phys. Lett.* **B 524**, 161 (2002); U. Mahanta and A. Datta, *Phys. Lett.* **B 483**, 196 (2000); U. Mahanta and S. Rakshit, *Phys. Lett.* **B 480**, 176 (2000); P. Das and U. Mahanta, hep-ph/0110309.
- [7] P. K. Das, hep-ph/0407041.
- [8] J. C. Collins, A. Duncan and S. D. Joglekar, *Phys. Rev.* **D 16**, 438 (1977).
- [9] See, for example, *Current Algebra and Anomalies*, by S. Treiman and R. Jackiw, Princeton University Press (1986).
- [10] P. K. Das, S. K. Rai and S. Raychaudhuri, *Phys. Lett.* **B 618**, 221 (2005).
- [11] A. Djouadi, hep-ph/0503172; J. F. Gunion, H. E. Haber, G. L. Kane and S. Dawson, *The Higgs Hunter Guide*, Addison-Wesley Publishing Company (1990).
- [12] G. B. Mohanty, Phd. Thesis, CERN (CERN Report No. CERN-THESIS-2004-025, 2002).
- [13] N. Arkani-Hamed, S. Dimopoulos and G. Dvali, *Phys. Lett.* **B 429**, 263 (1998); I. Antoniadis, N. Arkani-Hamed, S. Dimopoulos and G. Dvali, *Phys. Lett.* **B 463**, 257 (1998).
- [14] S. C. Park, H. S. Song and J. Song, *Phys. Rev.* **D 65**, 075008 (2002).
- [15] H. L. Lai *et. al.* (CTEQ Collaboration), *Phys. Rev.* **D 55**, 1280 (1997).